CONSENSUS CREDIBILITY PARTICLE FILTER FOR SPACE OBJECT TRACKING

Han Cai* **and Moriba Jah†**

Oden Institute for Computational Engineering and Sciences, The University of Texas at Austin, Austin, Texas 78712, USA

ABSTRACT

This paper exploits the formulation of a novel consensus credibility particle filter in the framework of Outer Probability Measures (OPMs) for space object tracking. Compared to the conventional probabilistic fusion method, the proposed method offers two advantages. First, by replacing the probability measures with OPMs, the credibility particle filter offers the ability to properly represent the epistemic uncertainty that comes from ignorance, such that all uncertain components in the estimation problem do not necessarily need to be modeled by probability distributions. Second, in order to overcome the limitation that the relative accuracy of local inputs is generally overlooked in the typical averaged consensus algorithm, a weighted consensus method is developed, where the fusion weight is adaptively determined based on the information gain of local estimates. This information-driven weighted consensus method can provide improved robustness and fast reduction of ignorance in the fusion process. The features of the method are validated via a space object tracking scenario using four real data sets, i.e., Planets Labs, LeoLabs, JSpOC, and ASTIRA.

Keywords: consensus fusion; outer probability measure.

1. INTRODUCTION

The Bayesian recursive estimation framework is the fundamental of many stochastic filtering methods for space object tracking. Typical Bayesian filtering methods assume various sources of uncertainty in a dynamical system are aleatoric or random, which can be well-represented by random variables and characterized by probability distributions. However, there is another class of uncertainty that comes from the lack of information is always overlooked in an estimation problem, and it is referred to as epistemic uncertainty. As oppose to aleatory uncertainty, which comes from the inherent randomness of the system, epistemic uncertainty is reducible if one can gain and process information to learn more aspects of the system. Representing epistemic uncertainty based on probability theory may lead to an inappropriate, ill-adapted quantification, and even produce potentially catastrophic operational implications in Space Situational Awareness (SSA) [1]. An example of this is the probability dilution phenomenon [2] in conjunction assessment, where the large covariance of two approaching objects reduces the risk of collision. To wit, probability dilution implies that the more ignorant we are the less probable a collision will occur. This false confidence is raised from the fundamental deficiency in the probabilistic representation of uncertainty [2].

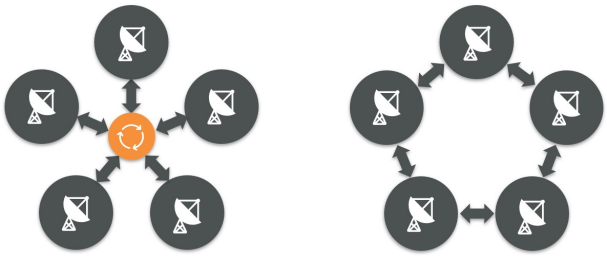

Figure 1: Schematic of the centralized and distributed sensor network

An appealing alternative to probability theory for uncertainty representation is the Outer Probability Measure (OPM) [3]. OPMs provide a faithful representation of epistemic uncertainty and it is able to properly account for the limited or imperfect information we possess of the system. Bayesian filtering solutions on the basis of OPMs [3, 4, 5], dubbed credibility filter, have been derived for a recursive "uninformative prior" Bayesian estimation. The major advantage of the credibility filter is that it is capable to handle the situation of ignorance or partial knowledge about the dynamical system. Recently, Sequential Monte Carlo (SMC) implementation of the credibility filter, namely Credibility Particle Filter (CPF), has been successfully applied to study the space object tracking problem [6, 7, 8].

As more and more space surveillance and tracking systems coming online, an increased amount of data from various astronomical sensors, e.g., radar, telescope, and laser ranging stations, are available for SSA research. One effective solution to achieve improved tracking performance is to fuse multiple data sets regarding the same

*Postdoc research fellow, Oden Institute for Computational Engineering and Sciences, caihanspace@gmail.com.

†Associate professor, Department of Aerospace Engineering and Engineering Mechanics

space object. Fusion techniques vary depending on the architecture of the sensor network. The left subfigure of Fig. 1 shows the topology of a centralized network. Accordingly, a centralized fusion method provides the best state estimation when all the sensors are accurately aligned [9]. Yet, the centralized method is generally unscalable and inefficient to the large-scale sensor network. Moreover, a fusion center is needed to collectively process measurements provided by all sensors, while the failure of the fusion center can be a catastrophe to the entire network. Alternatively, distributed fusion algorithms are able to provide a robust state estimation without utilizing a fusion center. As shown in the right subfigure of Fig. 1, each sensor node in a distributed sensor architecture only has access to the information from its neighborhood nodes, and none of them can directly acquire knowledge of the overall sensor network topology. For the particle filter, the commonly used distributed fusion method is the averaged consensus algorithm [10, 11, 12]. The crux of averaged consensus is to iteratively exchange information among neighborhood sensors until all of them reach an agreement on some consensus states. Several categories of averaged consensus algorithms have been developed, and two representatives are consensus on weight and consensus on posterior.

The principle of weight consensus is to maintain the same particle set at each sensor node and exchange the posterior particle weights within neighboring networks [13]. A prerequisite is that the filters running at all sensors are enforced to be highly synchronized. For instance, each local filter needs to have the same random number generator and the same state transition model to ensure the prior particle set at each sensor node is exactly the same [13]. However, synchronization across a space surveillance and tracking network is a challenging task, which prevents the generation of an identical particle set for achieving consensus. In addition, such a consensus method necessitates the transmission of the whole set of particle weights, while the number of particles is generally considerable high in order to deal with the particle depletion problem [6].

The method of consensus on posterior generally assumes a parametric representation of the posterior particle set as a Gaussian Probability Density Function (PDF) [10, 14] or Gaussian mixture model [15, 16]. The parameterization approach reduces the communication load compared to diffusing the whole set of particles in the network. In addition, consensus on posterior gives each sensor the flexibility to implement localized filtering schemes independently, which is more applicable in SSA. In addition, the averaged consensus method gives rise to a limitation that the relative accuracy of the local posteriors is generally ignored in the fusion process. Intuitively, the posterior consensus method aims to approach the arithmetic mean of all local posteriors. Hence, the fusion performance may be sensitive to biased local posterior caused by outliers or missed detection. Weighted consensus fusion method [17] is a feasible solution to this issue, while the assignment of fusion weight for improved performance still needs to be further investigated.

Motivated by these considerations, this paper presents a comprehensive study on consensus fusion leveraging the notion of OPMs. A weighted consensus CPF algorithm is developed, and to our knowledge, the method is the first distributed fusion algorithm that is fully derived based on the credibility framework. Compared to typical probabilistic consensus filters, the credibilistic consensus method can provide advanced performance in the absence of perfect dynamical and observation models. Moreover, instead of simply pursuing the arithmetic mean of local posteriors, the weighted consensus method adaptively tunes the fusion weight according to the credibilistic information gain of local posteriors. The information-driven weighting strategy can achieve improved robustness and fast reduction of ignorance in the fusion process. The developed method is validated using a real space object tracking case study, which considers the fusion of real orbit determination results from four data sets, i.e., Planets Labs, LeoLabs, JSpOC, and ASTIRA.

The rest of the paper is organized as follows. The fundamental of OPMs and credibility Bayesian filter is briefly introduced in Sec. 2. Sec. 3 summarizes the procedure of CPF and the implementation of averaged consensus credibility particle filter. In Sec. 4, the weighted consensus credibility particle filter is elaborated. The test and discussions are presented in Sec. 5. The last section concludes the paper.

2. BACKGROUND

The standard particle filter is derived based on the principle of sequential importance sampling, which is a fundamental Monte Carlo (MC) method for approximating integrals. According to Ref. [4], CPF is a generalization of the widely-used bootstrap particle filter in the OPM framework. The interpretation of CPF relies on the credibilistic implementation of Bayesian filtering methods. In this section, the fundamental of OPMs and the description of the multi-sensor credibility Bayesian filter are briefly reviewed.

2.1. OPMs and Possibility Functions

Outer probability measure is a special case of outer measure, which assumes the measure of the whole state space $\mathbb{X}$ equals to 1 and gives 0 to the empty set. For a subset A of the state space $\mathbb{X}$, the OPM $\bar{P}(A) \in [0, 1]$ indicates the credibility of the event $X \in A$, where X is referred to as an uncertain variable. Compared to the random variable in probability measure, the concept of uncertain variable is introduced to model both the aleatory and epistemic uncertainty of an uncertain system.

In contrast to probability measure, which is an intrinsic characterization of randomness, OPM defines the upper bound of the potential probability distribution that characterize the random behavior of the process. Hence, it

is also referred to as an extrinsic description of uncertainty. In addition, OPM is distinct from probability measure as it releases the additivity assumption and instead fulfills the subadditivity property, that is, $\bar{P}(A \cup B) \leq \bar{P}(A) + \bar{P}(B)$ for any subsets A and B.

The specific form of OPMs needs to be defined for deriving further applications, and the simplest OPM is given by [3]

$$\bar{P}(A) = \max_{x \in A} f(x), \tag{1}$$

where the non-negative function $f \to [0, 1]$ is a possibility function that describes the uncertain variable x. Theoretically, the definition of possibility function is the same as the possibility distribution in possibility theory, and OPM can also be referred to as possibility measure [18].

The commonly used Gaussian possibility function is defined by

$$\bar{\mathcal{N}}(x; \mu, S) = \exp\Big(-\frac{1}{2}(x-\mu)^T S^{-1}(x-\mu)\Big), \tag{2}$$

for some $\mu \in \mathbb{R}^d$ and some $d \times d$ positive definite matrix S, where μ and S are defined as probabilistic mean and variance, respectively. The probabilistic counterpart of the mean μ represents a state that is statistically most likely, while the possibilistic mean μ does not have the same statistical property, and it instead implies a state that all evidence has not discarded. The possibilistic variance S describes the spread of the function.

A Gaussian possibility function can be easily turned into a Gaussian PDF by multiplying a scaling parameter $1/\sqrt{|2\pi S|}$. However, the Gaussian PDF characterizes the randomness of the process, while a Gaussian possibility function presents a representation of the total amount of information available to us, or more intuitively, it can be interpreted as a Gaussian-shaped upper bound for the uncertainty.

2.2. Multi-Sensor Credibility Bayesian Filter

Consider an SSA network consists of N sensors that jointly observing a space object. Supposing the characteristics of the orbital motion is not well-known, and the state of the target of interest can be modeled by an uncertainty variable x. The state evolution model at time t_k is described by a possibility function F, i.e.,

$$x_k = F\big(x_{k-1},\, Q_k\big). \tag{3}$$

In the context of SSA, F is a function of orbital dynamics and the uncertain variable Q_k is the process noise that models the imperfection of the dynamic models employed in the propagator. Similarly, modeling the observation as an uncertain variable denoted by z_k, then, the observation model of sensor n is given by

$$z_k^n = H_k^n\big(x_k, R_k^n\big), \tag{4}$$

where H^n denotes the function of the observation process of sensor n. The observation noise R_k^n is an uncertain variable representing the imperfect information embedded in the observation process of sensor n, and it is assumed independent across the sensor network in this paper. The measurements of all sensors can be summarized in a matrix $z_k = [z_k^1, \cdots, z_k^N]$, and the observation function of all sensors is defined by $H_k = [H_k^1, \cdots, H_k^N]$.

In the case where all sensor measurements z_k are available to a fusion center, a credibility Bayesian filter can be implemented to process all measurements in a centralized manner. Following the derivation of Refs. [3, 4], a credibility Bayesian filter yields the same predict-update recursion if all possibility functions are Gaussian. Supposing the information of the target state at epoch t_{k-1} is modeled by a posterior possibility function f_{k-1}, the prior possibility function at epoch t_k is calculated using the the following prediction equation

$$f_{k|k-1}(x|z_{1:k-1}) = \sup_{x' \in \mathbb{X}_{k-1}} m(x|x') f_{k-1}(x'|z_{1:k-1}), \tag{5}$$

where the conditional possibility function m describes the transition of the object's state from time $k-1$ to k. The prediction formula is the analog of the Chapman-Kolmogorov equation used in the standard Bayesian estimation method, while the integral is replaced by supremum.

The prior possibility function $f_{k|k-1}(x|z_{1:k-1})$ can then be updated by the information contained in the new observations z_k of all sensors based on Bayesian inference, the resultant posterior possibility function at time t_k is given by

$$f_k(x|z_{1:k}) = \frac{l(z_k|x) f_{k|k-1}(x|z_{1:k-1})}{\sup\limits_{x' \in \mathbb{X}_k} l(z_k|x') f_{k|k-1}(x'|z_{1:k-1})}. \tag{6}$$

The update equation takes a similar form as the Bayes' theorem, but the integral is replaced by supremum, and the global likelihood function $l(z_k|x)$ is a possibility function, which can be factorized into a product of local likelihood functions

$$l(z_k|x_k) = \prod_{n=1}^{N} l(z_k^n|x_k). \tag{7}$$

3. CONSENSUS CREDIBILITY PARTICLE FILTER

In this section, the credibility particle filter is first summarized in Sec. 3.1, following by the averaged consensus implementation of the credibility particle filter presented in Sec. 3.2.

3.1. A Summary of the Credibility Particle Filter

Standard particle filters suffer from the particle degeneracy issue, meaning that a large portion of particles will have negligible weight after a few iterations of recursive estimation. The degeneracy issue is particularly severe in a space object tracking scenario, especially when the sensors are accurate and/or the measurements are too sparse. Several approaches have been developed to deal with this issue, e.g., data adaption method [13], unscented particle filter [19], particle Gaussian mixture filter [20, 21].

In this paper, a parametric representation approach is applied to approximate the prior SMC set as a Gaussian possibility function, such that an unscented Kalman filter update step can be performed instead of the standard importance weight update. Posterior particles can be reallocated to high likely state space through sampling from the posterior Gaussian possibility function. The proposed CPF preserves the non-linear uncertainty propagation property of the particle filter and enables an unscented Kalman update to cope with the particle degeneracy problem. The detailed procedure of CPF is outlined as the following steps.

- **Initialization**

  Suppose the information of the initial orbit state is modeled as an OPM that approximated by a set of weighted particles $\{(w_0^j, x_0^j)\}_{j=1}^M$, and the particle set is normalized with maximum weight equals one, i.e., $\max_{1\le j\le M} w_0^j = 1$. The initial OPM is given by

$$\bar{P}_0(x) = \max_{1\le j\le M} w_0^j \delta_{x_0^j}(x), \tag{8}$$

  where $\delta_X(Y)$ is the Kronecker delta function with $\delta_X(Y) = 1$ if and only if $x = Y$ and $\delta_X(Y) = 0$ otherwise.

- **Prediction**

  Given the posterior OPM $\bar{P}_{k-1}$ represented by a set of particles $\{(w_{k-1}^j, x_{k-1}^j)\}_{j=1}^M$, the prior OPM $\bar{P}_{k|k-1}$ at epoch t_k is approximated by the particle set $\{(w_{k|k-1}^j, x_{k|k-1}^j)\}_{j=1}^M$ based on Eq. (5). The state and weight of the jth particle is given by

$$x_{k|k-1}^j \sim p_c(m(x_{k|k-1}^j | x_{k-1}^j)), \tag{9}$$

$$w_{k|k-1}^j = \frac{w_{k-1}^j m(x_{k|k-1}^j | x_{k-1}^j)}{\max_{1\le i\le M} w_{k-1}^j m(x_{k|k-1}^j | x_{k-1}^j)}. \tag{10}$$

  The state transition function m is a conditional possibility function $\bar{\mathcal{N}}(x_{k|k-1}^j; o_k(x_{k-1}^j), Q_k)$, where o_k represents the orbit propagator. Note that one cannot sample from a possibility function directly, and $p_c(m)$ represents a PDF approximation of the state transition function m based on the maximum-entropy principle [4]. The prediction step yields the prior OPM expressed as follows

$$\bar{P}_{k|k-1}(x) = \max_{1\le j\le M} w_{k|k-1}^j \delta_{x_{k|k-1}^j}(x). \tag{11}$$

- **Parameterization**

  Instead of taking the statistical mean and covariance of the prior particles $\{(w_{k|k-1}^j, x_{k|k-1}^j)\}_{j=1}^M$, a Gaussian possibility function $\tilde{f}_{k|k-1}$ is constructed as the minimal bound of their weights, i.e.,

$$\{(w_{k|k-1}^j, x_{k|k-1}^j)\}_{j=1}^M \to \tilde{f}_{k|k-1}(x), \tag{12}$$

  where $f_{k|k-1}(x) = \bar{\mathcal{N}}(x; \mu_{k|k-1}, S_{k|k-1})$, and the parameters $\mu_{k|k-1}$ and $S_{k|k-1}$ are estimated through an optimization process detailed in our earlier work [22]. This approximation preserves the information carried by the particle set.

- **Update**

  Measurement update of a Gaussian possibility function follows the standard unscented Kalman filter update step. We first generate a set of sigma points $\{\boldsymbol{\chi}_k^i\}_{i=0}^{2d}$ of the Gaussian possibility function as follows:

$$\boldsymbol{\chi}_k^i = \left[\mu_{k|k-1}^i,\ \mu_{k|k-1}^i \pm \left(\sqrt{d+\lambda} G_{k|k-1}\right)^i\right], \tag{13}$$

  where $G_{k|k-1} = \text{chol}(S_{k|k-1})$ is the Cholesky factorization of the prior covariance, d is the dimension of the state, λ is a scaling parameter. The expected measurement $\hat{z}_k$, measurement variance $S_{k,z}$, and cross-variance $S_{k,xz}$ are calculated via the unscented transform method as:

$$\hat{z}_k = \sum_{i=0}^{2d} W^i \boldsymbol{\gamma}_k^i, \tag{14}$$

$$S_{k,z} = \sum_{i=0}^{2d} W^i (\boldsymbol{\gamma}_k^i - \hat{z}_k)(\boldsymbol{\gamma}_k^i - \hat{z}_k)^T + R_k, \tag{15}$$

$$S_{k,xz} = \sum_{i=0}^{2d} W^i (\boldsymbol{\chi}_i - \mu_{k|k-1}^i)(\boldsymbol{\gamma}_k^i - \hat{z}_k)^T, \tag{16}$$

  where the sigma points $\{\boldsymbol{\gamma}_k^i\}_{i=0}^{2d}$ are generated using the predicted sigma points and the observation function: $\boldsymbol{\gamma}_k^i = H_k(\boldsymbol{\chi}_k^i)$. The weights $W^i = \delta_0(i)\frac{\lambda}{d+\lambda}$ if $i = 0$, and $W^i = \frac{\lambda}{2(d+\lambda)}$ otherwise.

  The updated mean μ_k and variance S_k are given by

$$\mu_k = \mu_{k|k-1} + K_k(z_k - \hat{z}_k), \tag{17}$$

$$S_k = S_{k|k-1}^l + K_k S_{k,z} (K_k)^T, \tag{18}$$

  where the Kalman gain is $K_k = S_{k,xz}(S_{k,z})^{-1}$. The update step provides a posterior Gaussian possibility function with the form $\tilde{f}_k(x) = \bar{\mathcal{N}}(x; \mu_k, S_k)$.

- **SMC Recovery**

  To proceed with the next iteration of the particle filter, a set of samples $\{(w_k^j, x_k^j)\}_{j=1}^M$ are drawn from the maximum entropy PDF [4] of the posterior

Gaussian possibility function. The state and weight of a sample are given by

$$x_k^j \sim \mathcal{P}_c(\tilde{f}_k(x)),$$
$$w_k^j = \frac{\tilde{f}_k(x_k^j)}{\max\limits_{1\le j'\le n} \tilde{f}_k(x_k^{j'})}. \tag{19}$$

The resultant particle set forms the posterior OPM, i.e.,

$$\bar{P}_k(x) = \max_{1\le j\le M} w_k^j \delta_{x_k^j}(x). \tag{20}$$

The commonly used state estimation method in a typical particle filter is the Maximum *A Posteriori* (MAP) method. In the credibilistic MAP estimate, the state of the particle with the maximum posterior weight is taken as the best state estimation, that is $\hat{x}_k = x_k^\tau$, where $\tau = \arg\max_j w_k^j$.

Remark 1. Theoretically, a Gaussian possibility function is able to bound many probability distributions, meaning that the parameterization method is applicable even if the prior does not follow a Gaussian distribution. In the case when the prior is multi-modality, a more reasonable alternative is to approximate the prior as a Gaussian max-mixture using a clustering method. However, this approach introduces additional difficultly for the following consensus fusion process. The fusion of two Gaussian max-mixtures has not been conducted in literature according to our knowledge. Developing an effective fusion rule for Gaussian max-mixtures will be studied in future research.

3.2. Averaged Consensus Credibility Particle Filter

The CPF presented in the above section is implemented in a centralized fashion, which achieves optimal estimation accuracy by collectively integrating the knowledge from all sensor nodes. In this section, an averaged consensus credibility particle filter, namely AC-CPF, is presented for the use of more practical distributed SSA networks. The parametric representation in CPF improves the efficiency of the consensus fusion. Specifically, the communication cost of broadcasting two quantities, possibilistic mean and variance, through the network is significantly lower than transmitting a set of particles. In addition, the parametric representation approach is more applicable in engineering practice since it releases the requirement of synchronization between local filters.

The communication topology of a distributed network can be represented by a Graph $\mathcal{G} = \{\mathcal{V}, \mathcal{E}\}$, where $\mathcal{V} = \{1, \cdots, N\}$ is a vertex set with each represents a sensor node, and $\mathcal{E} \subset \mathcal{V} \times \mathcal{V}$ represents the edge set, which models the communication links between sensors. An edge set $\mathcal{E}(m, n)$ denotes that sensor m and n can communicate with each other. The edge set can be time-variant, while it is assumed as a constant matrix in this paper for brevity.

The update step of each localized CPF yields a local posterior that is updated based on its own measurement. The task of consensus fusion is to determine a global posterior to every sensor. The consensus states are the posterior mean μ_k and variance S_k. Based on the consensus rule, sensor n updates its consensus states by iterating the averaged consensus equations, i.e.,

$$\mu_k^n(i) = \beta_{n,n}\mu_k^n(i-1) + \sum_{m\in N_n} \beta_{n,m}\mu_k^m(i), \tag{21}$$

$$S_k^n(i) = \beta_{n,n}S_k^n(i-1) + \sum_{m\in N_n} \beta_{n,m}S_k^m(i), \tag{22}$$

where i indicates the index of iteration, N_n denotes the neighborhood nodes of sensor n with n excluded. A popular choice of the fusion weight $\beta_{n,m}$ is the Metropolis weight [23]:

$$\beta_{n,m} = \begin{cases} \frac{1}{1+\max\{|N_n|,|N_m|\}} & \text{if } (n,m)\in\mathcal{E} \\ 1 - \sum_{(n,m)\in\varepsilon} \beta_{n,m} & \text{if } n = m \\ 0 & \text{otherwise,} \end{cases} \tag{23}$$

where $|N_n|$ represents the degree or cardinality of sensor n. If the communication graph remains connected, and the fusion weight matrix $B = [\beta_{n,m}]_{N\times N}$ is primitive and doubly stochastic, then the consensus method achieves the sample mean of the consensus states asymptotically as the number of iteration tends to infinity [23], that is

$$\lim_{i\to\infty} \mu_k^n(i) = \frac{1}{N}\sum_{n=1}^{N} \mu_k^n(0), \tag{24}$$

$$\lim_{i\to\infty} S_k^n(i) = \frac{1}{N}\sum_{n=1}^{N} S_k^n(0). \tag{25}$$

Also, it has been proved that a global consensus can be achieved in a finite number of iterations [13, 16].

The procedure of the AC-CPF is shown as the flowchart in Fig. 2. The overall process of AC-CPF is similar to the centralized CPF, while only the consensus fusion step requires communication among neighboring nodes and all remaining steps can run locally.

The output of the averaged consensus method is a global posterior Gaussian possibility function across the network. Determining a global posterior particle set is possible, whereas this requires either another circle of distributed communication or a common random seed generator to achieve synchronization on the particles. In this paper, the posterior mean of the global posterior is taken as the state estimation. This enables the SMC recovery step to run locally without extra synchronization operations.

4. WEIGHTED CONSENSUS CREDIBILITY PARTICLE FILTER

The major drawback of the AC-CPF method is that the fusion process does not take into account the relative ac-

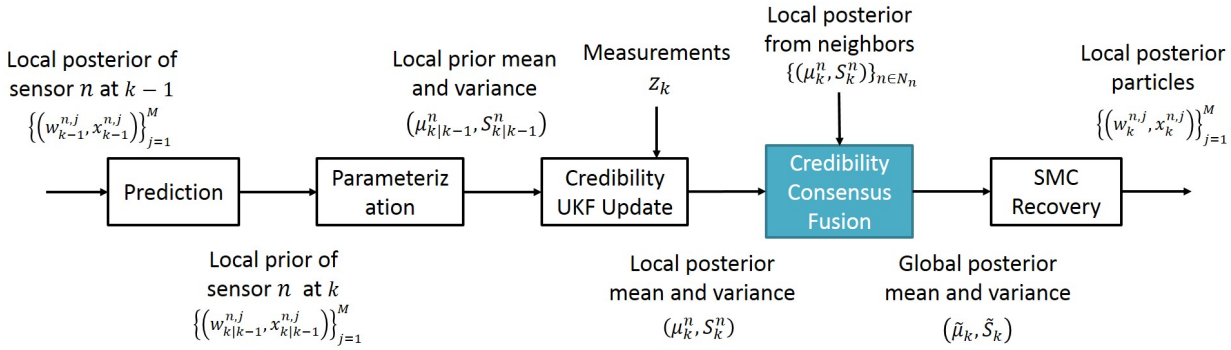

Figure 2: Flowchart of the consensus credibility particle filter

curacy of local information. Thus, the algorithm is sensitive to biased local estimations and may yield poor performance when some low-precision sensors are involved in the network. To address this issue, a Weighted Consensus Credibility Particle Filter (WC-CPF) is developed, in which the fusion weight is adaptively determined according to the information content carried by local measurements. In general, more informative measurements indicating more accurate state estimation [24], and the information content carried by measurements is proportional to the information gain of replacing the prior by the posterior. Hence, it is expected that weighting each local posterior based on its information gain can achieve an improved accuracy than simply taking the averaged consensus. The principle of information-driven fusion strategy has been investigated in Refs. [25, 26] to address the multi-sensor multi-target tracking problem. The WC-CPF method presented in this section is derived within the framework of OPMs, which is fundamentally different from the state of the art. To implement WC-CPF, two research questions need to be resolved. The first is to determine the uncertainty of a possibility function, and the second is to quantify the information gain between the prior and local posterior. Feasible solutions to these two questions are presented in the following sections.

4.1. Credibility Information Gain

The overwhelming approach for measuring uncertainty in probability theory is Shannon entropy or entropy for brevity. The entropy of a random variable measures the expected amount of information on its possible outcomes. For a probability distribution, its uncertainty is considered as equivalent to the information content in general. The concept of entropy is designed for probability measure, and adapting it to OPMs is less applicable. A possibilistic counterpart of the Shannon entropy, namely U-uncertainty is derived in Ref. [27]. The information closeness of possibility functions based on the U-uncertainty is presented in Ref. [28]. The U-uncertainty and information gain function for possibility functions are briefly discussed in this section.

Uncertainty of Possibility Functions

Given a finite set $X = \{x_1, \cdots, x_m\}$ and a possibility function f, the possibility value of the ith point is $w_i = f(x_i)$, $i \in N_m$, so we can define a discrete possibility function as follows

$$\tilde{f} = (w_1, \cdots, w_n) \in \mathcal{F}, \tag{26}$$

where $\mathcal{F}$ denotes the set of possibility functions with at least one non-zero element. The information of each discrete possibility function can be summarized in a level set L_f, that is

$$L_f = \{\ell \mid (\exists i \in N_m)(w_i = \ell) \text{ or } \ell = 0\}. \tag{27}$$

Each element ℓ in L_f represents a unique possibility value in $\tilde{f}$. Further, the level set is defined in ascending order: $L_f = \{\ell_1, \cdots, \ell_r\}$, where $\ell_1 = 0$, for any $i < j$, $\ell_i < \ell_j$, and $r = |L_f|$ in general. The maximum level of the set is denoted as $\ell_f = \max_i w_i$.

Given a discrete possibility function and its level set, its credibility uncertainty is defined by the U-uncertainty [27]

$$U(\tilde{f}) = \frac{1}{\ell_f} \sum_{i=1}^{r-1} (\ell_{i+1} - \ell_i) \log_2 |c(f, \ell_{i+1})|, \tag{28}$$

where $c(f, \ell)$ is a ℓ-cut function, and

$$c(f, \ell) = \{i \in N_m | w_i \geq \ell\}. \tag{29}$$

This ℓ-cut function consists of all the possibility values greater than or equal to a level ℓ, and $|c(f, \ell)|$ denotes the cardinality of this set.

Eq. (28) can also be rewritten as a form of integration as follows

$$U(\tilde{f}) = \int_0^1 \log_2(c(f, \ell)) \mathrm{d}\ell. \tag{30}$$

However, it is intractable to numerically solving Eq. (30) for a continuous possibility function. To adapt the method to measure the uncertainty of continuous possibility functions, a sampling procedure is first required to discrete the possibility function as a finite set. Given a Gaussian possibility function $f_0 = \mathcal{N}(x; \mu_0, S_0)$, the

discretization is achieved by generating a set of m samples $\{x_i\}_{i=1}^m$ from a PDF $\mathcal{P}_c(f_0)$ that generated as the maximum entropy approximation [4] of f_0. The possibility values of the samples form the associated discrete possibility function $\tilde{f}_0 = \{w_i = f_0(x_i)\}_{i=1}^m \cup 0$ with 0 included. A discrete possibility function needs to be normalized, i.e., $\max_i w_i = 1$, before the computation of the U-uncertainty. The level set L_{f_0} is generated and sorted in ascending order. The U-uncertainty can then be calculated using Eq. (28).

Information Gain of Possibility Functions

Following the definition in Ref. [28], given two possibility functions f_1 and f_2, if their discrete possibility functions are comparable and $\tilde{f}_1(x) \leq \tilde{f}_2(x)$ for all $x \in X$, the information gain of replacing $\tilde{f}_2$ by $\tilde{f}_1$ is the Euclidean distance between their U-uncertainties, that is

$$g(\tilde{f}_1, \tilde{f}_2) = U(\tilde{f}_2) - U(\tilde{f}_1). \tag{31}$$

As $\tilde{f}_1(x) \leq \tilde{f}_2(x)$, it is straightforward to conclude that $g(\tilde{f}_1, \tilde{f}_2)$ is non-negative, and $g(\tilde{f}_1, \tilde{f}_2) = 0$ if and only if $\tilde{f}_1 = \tilde{f}_2$.

Eq. (31) is valid if two possibility functions are comparable with each another, e.g., $\tilde{f}_1 \leq \tilde{f}_2$ or $\tilde{f}_1 \geq \tilde{f}_2$, $\forall x \in X$. Theoretically, two Gaussian possibility functions are comparable only if they have the same mean value, which prevents the application of Eq. (31) in practice. In the Bayesian estimation framework, the prior Gaussian possibility function is generally not comparable with the posterior PDF since they have different mean values. Therefore, their information gain cannot be calculated using Eq. (31).

To calculate the information gain of two possibility distributions without comparability, it is useful to define the joint distribution $\tilde{f}_1 \vee \tilde{f}_2$ as follows:

$$(\tilde{f}_1 \vee \tilde{f}_2)(x) = \tilde{f}_1(x) \vee \tilde{f}_2(x), \forall x \in X, \tag{32}$$

where $\tilde{f}_1(x) \vee \tilde{f}_2(x) = \max(\tilde{f}_1(x), \tilde{f}_2(x))$.

Based on the above definition, a new distance metric $G(\tilde{f}_1, \tilde{f}_2)$ is introduced as follows [28]

$$G(\tilde{f}_1, \tilde{f}_2) = g(\tilde{f}_1, \tilde{f}_1 \vee f_2) + g(\tilde{f}_2, \tilde{f}_1 \vee \tilde{f}_2). \tag{33}$$

Let $\tilde{f}_3 = \tilde{f}_1 \vee \tilde{f}_2$, the distance metric can be rewritten as

$$\begin{aligned} G(\tilde{f}_1, \tilde{f}_2) &= g(\tilde{f}_1, \tilde{f}_3) + g(\tilde{f}_2, \tilde{f}_3) \\ &= 2U(\tilde{f}_3) - U(\tilde{f}_1) - U(\tilde{f}_2). \end{aligned} \tag{34}$$

Unlike Eq. (31), which measures the information gain of replacing a possibility distribution by another, Eq. (33) reflects the variation on the information content, but does not indicates whether the information is gained or lost. A proper interpretation of Eq. (33) is that it assesses the information variation or information closeness of the given possibility distributions. In general, the information variation between the prior and posterior possibility functions can also be seen as the information gain of the posterior obtained through measurements. Therefore, it is reasonable to employ Eq. (33) for evaluating the information gain in a Bayesian estimation framework.

Finally, considering a Bayesian estimation process, and let the information gain of the posterior f_k with respect to the prior $f_{k|k-1}$ be $I(f_k, f_{k|k-1})$, then we have

$$I(f_k, f_{k|k-1}) = \begin{cases} g(\tilde{f}_k, \tilde{f}_{k|k-1}) & \text{if } \tilde{f}_k \leq \tilde{f}_{k|k-1} \\ G(\tilde{f}_k, \tilde{f}_{k|k-1}) & \text{otherwise.} \end{cases} \tag{35}$$

The calculation of the U-uncertainty and information gain of Gaussian possibility functions is illustrated using the following example.

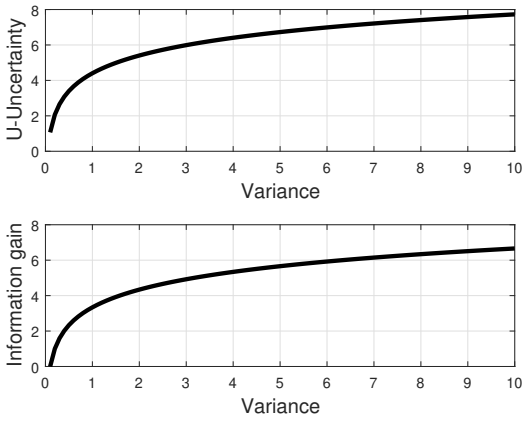

Figure 3: Examples of U-uncertainty and information gain

The top subfigure in Fig. 3 shows the U-certainty of Gaussian possibility functions with zero mean, but different variance values ranging from 0.1 to 10. In order to perform a fair comparison, the uncertainty is calculated using 1000 uniformly distributed samples. Clearly, the larger variance value yields a higher uncertainty level.

To illustrate the information gain function, the information closeness between a Gaussian possibility function $\mathcal{N}(x; 0, 0.1)$ and a set of Gaussian possibility functions $\mathcal{N}(x; 0, S)$ with variance values ranging from 0.1 to 10 is calculated. The result shown in the bottom subfigure of Fig. 3 is as expected, where the information divergence between the two functions is proportional to the variance value.

4.2. Weighted Consensus Credibility Particle Filter

This section introduces the implementation of WC-CPF. The overall procedure is similar to AC-CPF as the flowchart shown in Fig. 2, and the major difference is the way to design the fusion weight.

The fusion weight $\beta_{n,m}$ in Eq. (23) is computed based on the credibilistic information gain at each sensor node. Specifically, the prior $f^n_{k|k-1}$ and posterior f^n_k of sensor node n are discretized as possibility distributions following the description given in Sec. 4.1. The information gain $I(f^n_{k|k-1}, f^n_k)$ can then be calculated using Eq. (35). Let $I(f^n_{k|k-1}, f^n_k)$ of sensor n at epoch k be I^n_k for simplicity, the WC-CPF method is achieved by replacing the Metropolis weight by the following information-driven weights

$$\beta_{n,m} = \begin{cases} \frac{I^m_k}{I^n_k + \sum_{(n,m)\in\varepsilon} I^m_k} & \text{if } (n,m) \in \mathcal{E} \\ 1 - \sum_{(n,m)\in\varepsilon} \beta_{n,m} & \text{if } n = m \\ 0 & \text{otherwise.} \end{cases} \tag{36}$$

It has been proved that if the fusion weight matrix $B = [\beta_{n,m}]_{N\times N}$ is primitive and row stochastic, then the consensus states can asymptotically converge to the weighted arithmetic mean of the given inputs [17], i.e.,

$$\lim_{i\to\infty} \mu^n_k(i) = \sum_{m=1}^{N} \beta_{n,m} \mu^m_k(0), \tag{37}$$

$$\lim_{i\to\infty} S^n_k(i) = \sum_{m=1}^{N} \beta_{n,m} S^m_k(0). \tag{38}$$

Compared to the averaged consensus fusion approach, WC-CPF requires further computational effort to calculate the information gain at each local node, but it does not yield additional communicational load to the consensus process. The information-driven weighting method is able to automatically assign more weights to local posteriors that are updated by more informative measurements. The fusion weight of a local posterior without measurement update is exactly equaled to zero since no information is gained. In such a scenario, the information gain is assumed as a small value, e.g., $I^n = 0.01$ in order to avoid totally abandon this local information from the fusion process.

5. TEST AND DISCUSSION

To illustrate the proposed method, a case study of consensus fusion is presented in this section. The scenario considers the fusion of some real orbit determination results provided by four space object catalog using the consensus fusion method. These orbital states can be interpreted as human "opinions" since the absence of sufficient statistical information to characterize their accuracy.

5.1. Test Design

The consensus fusion of orbit determination results from multiple data providers, i.e., Planet Labs, LeoLabs, JSpOC, and ASTRIA is studied. Each data provider maintains a space object catalog to provide a timely updated 6-dimensional orbit state based on their own observations. Specifically, the orbital estimations provided by Planet Labs, LeoLabs, and JSpOC are generated using GPS data, radar measurements, and TLE data, respectively. Orbital estimation from ASTRIA is generated by jointly processing LeoLabs' radar measurements using the unscented Kalman filter.

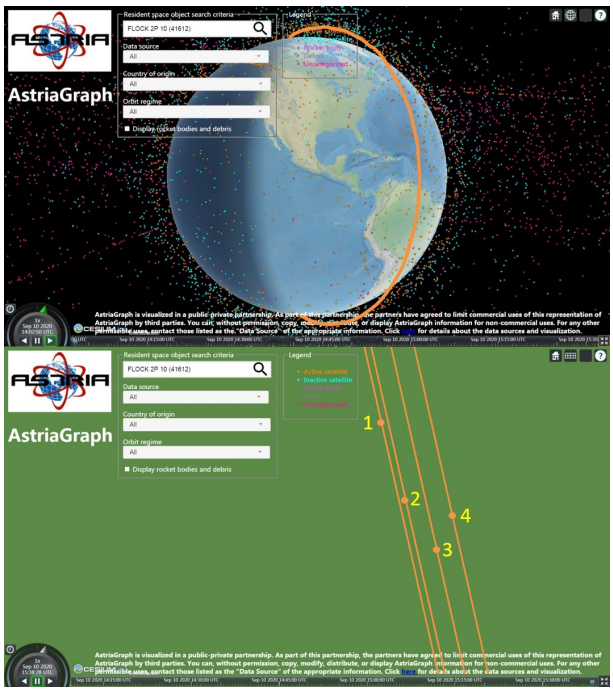

Figure 4: Orbit determination results of 0E2F shown in ASTRIAGraph

The tested target is a Flock 2P satellite: 0E2F (the corresponding NORAD ID assigned by the USSTRATCOM is 41612) operated by Planet Labs. Orbit determination results of 0E2F by the 4 data providers can be visualized in ASTRIAGraph[1]. The top subfigure of Fig. 4 is a screenshot of the ASTRIAGraph, where the colorful dots surrounding the Earth shows the crowded environment of outer space, and the orange curve actually represents the 4 osculating orbits of 0E2F, while they are too close to be distinguished. The bottom subfigure is an enlarged plot, where the four orange curves with labels from 1 to 4 represent the orbits determined by JSpOC, Planet Labs, LeoLabs, and ASTRIA, respectively, and the dot in each curve is the position of 0E2F at some epoch. Clearly, the difference between these 4 orbits is striking. By using these results for decision-making, e.g., sensor tasking, collision avoidance maneuver, may lead to conflicting results. This confusion, however, can be eliminated by using the consensus algorithm to achieve an agreement among different orbits.

Note that each data provider can only update one to two

[1]ASTRIAGraph is an interactive visualization application for space traffic monitoring, space safety, and sustainability. http://astria.tacc.utexas.edu/ASTRIAGraph/

orbital estimations of a target every day. Determining accurate tracking and fusion results based on such sparse data points is extremely challenging. Therefore, an interpolation method is utilized to generate a set of virtual orbital estimates by propagating a real orbit forward to some epoch that synchronized across the network until the next real orbit is available.

The fusion process starts from May 2, 2020 00:00:00 (UTC) to May 3, 2020 20:30:00 (UTC). Orbital states are assumed to be generated every 10 min, 30 min, and 60 min. The ground truth is obtained by using a batch least-squares method to process both GPS and radar data. A high-fidelity orbit propagator is considered, which employs perturbation models of 20×20 Earth gravitational field, MSIS00 atmospheric drag, solar radiation pressure assuming the objects are spherical with an area-to-mass ratio of $1.5\times10^{-3}\mathrm{m}^2/\mathrm{kg}^{-1}$, and lunisolar third-body perturbations. The process noise Q_k at each local node is a diagonal variance matrix with the variance defined as 10 m and 0.1 m/s for position and velocity respectively.

The filtering orbit states are modeled by the inertial position and velocity, and the initial filtering state of the target is generated by adding a zero-mean Gaussian noise to the truth. The standard deviation of the noise is approximately 10 km and 1 m/s for position and velocity, respectively. The initial variance of the target is the same as the standard deviation value. The uncertainty of different data sets is assessed using a training process prior to the filtering period. The approach is to model the discrepancy of two conserved quantities that determines the trajectory of a space object, namely the specific angular momentum and specific orbital energy. The detailed credibilistic uncertainty quantification approach can be found in Refs. [6, 7].

Three fusion methods, WC-CPF, AC-CPF, and centralized CPF, are compared using the same measurements and filtering parameters. The topology of the centralized and distributed SSA network is shown in Fig. 5, where each data provider is modeled as a local sensor node. In the centralized network, there is a CPF running at the fusion center to process all the local posteriors from the four sensor nodes. From the perspective of sensor network architecture, all sensors are assumed to have a common FOV and the target is able to appear at the FOV multiple times within the filtering period.

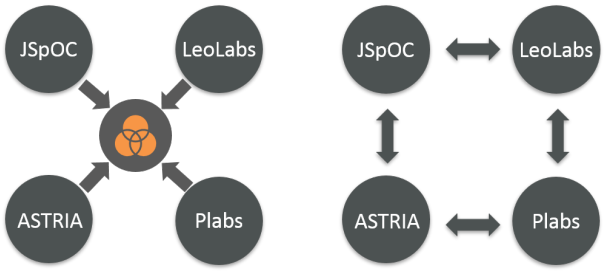

Figure 5: Schematic of the centralized and distributed sensor network (Plabs stands for Planet Labs)

5.2. Results

The accuracy of the WC-CPF, AC-CPF, and centralized CPF methods are validated by taking the averaged position error over 50 MC runs. The test results are drawn in Fig. 6. As we can see from the first three subfigures, although the three fusion methods can ultimately achieve a similar accuracy, their performance during the tracking time period is distinct. The centralized fusion achieves the most accurate and stable orbital state estimation among the three methods, and it is able to yield the same level of accuracy regardless of differences in the density of measurements. The results of WC-CPF in the three figures demonstrate that it can provide a similar performance to the centralized approach, especially when the measurements are not too sparse. The AC-CPF method, however, yields the worst accuracy in all the three subfigures. The difference between WC-CPF and AC-CPF is more evident as the increase of the time interval between measurements, see Figs. 6b and 6c.

The error of both AC-CPF and WC-CPF increases at the first half of the tracking. This can be illustrated by the error of the four data sources. Fig. 7 shows the position error in the case of 30 min. The measurement errors of the other two cases are omitted as they have a similar tendency. JSpOC's TLE data yields a large position error, and the magnitude is consistent with the solution given in Refs. [6], where the uncertainty quantification of the specific orbital energy suggest dozens of kilometers offset in the semi-major axis component. Furthermore, the measurements of Planet Labs show a rapid increase at the first half of the time window, while the measurement error at the second half is relatively small. Given these measurement errors, the tracking results validated that the WC-CPF method is able to adaptively reduce the fusion weight of local estimations with large measurement noise, and therefore outperforms the AC-CPF in terms of robustness for sensors with different noise profiles.

6. CONCLUSION

In this paper, a novel consensus fusion method, called Averaged Consensus Credibility Particle Filter (AC-CPF), is developed leveraging the notion of Outer Probability Measures (OPMs). This method provides the capability to handle the situation of ignorance or imperfect information in the fusion problem. On the basis of AC-CPF, a Weighted Consensus CPF (WC-CPF) method is further developed, where the fusion weight is automatically adjusted based on the credibilistic information gain of local posteriors. The information-driven weighting method is able to lead to a fast reduction of ignorance. A real-world test scenario using orbit determination results from 4 data sets, i.e., Planet Labs, LeoLabs, JSpOC, and ASTRIA is presented. Results demonstrated that the AC-CPF method performs well when a sufficient number of measurements are available for analysis, and the WC-CPF method is more robust to sparse measurement sce-

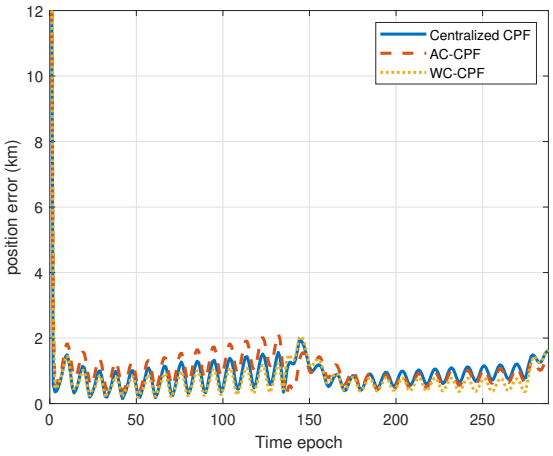

(a) 10 min

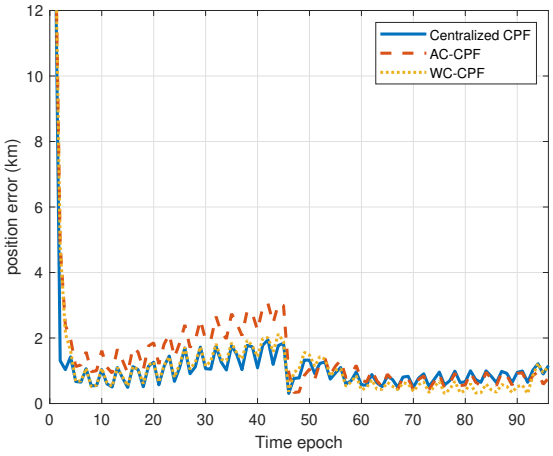

(b) 30 min

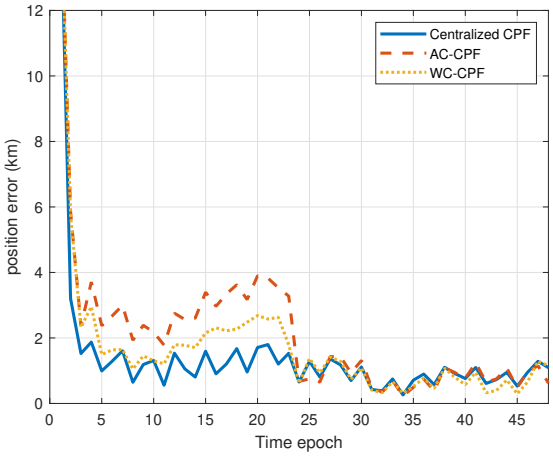

(c) 60 min

Figure 6: Position error using orbit determination results

narios and it can yield similar performance compared to the centralized fusion results.

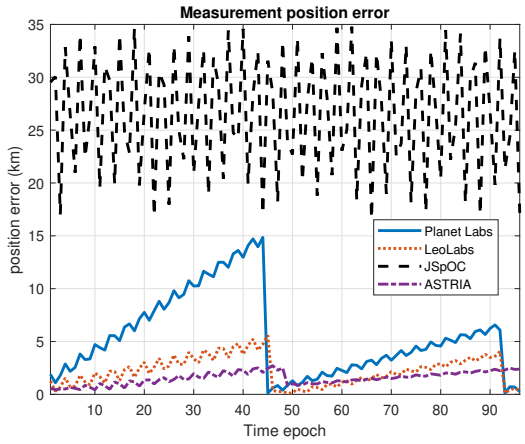

Figure 7: Measurement error

ACKNOWLEDGEMENT

This work was supported by the Air Force Office of Scientific Research (project number: FA9550-18-1-0351). The authors would like to acknowledge Dr. Emmanuel Delande and Dr. Jérémie Houssineau for the valuable discussion.

REFERENCES

1. Cai H., Hussein I., and Jah, M., (2020). Possibilistic admissible region using outer probability measure theory, *Acta Astronautica*, **177**, 246-257
2. Delande E., Jah M., and Jones B., (2019). A New Representation of Uncertainty for Collision Assessment, *AIAA/AAS Astrodynamics Space Flight Mechanics Meeting*, 19-452
3. Houssineau J., and Bishop A., (2018). A. Smoothing and filtering with a class of outer measures, *SIAM/ASA Journal on Uncertainty Quantification*, **6**(2), 845–866
4. Houssineau J. and Ristic B., (2017). Sequential Monte Carlo algorithms for a class of outer measures, arXiv preprint arXiv:1708.06489
5. Ristic B., Houssineau J., and Arulampalam S., (2018). Robust target motion analysis using the possibility particle filter, *IET Radar, Sonar & Navigation*, **13**(1) 18-22
6. Delande E., Houssineau J., and Jah M., (2018). Physics and human-based information fusion for improved resident space object tracking, *Advances in Space Research*, **62**(7), 1800-1822
7. Delande E., Houssineau J., and Jah M., (2018). A New Representation of Uncertainty for Data Fusion in SSA Detection and Tracking Problems, *2018 21st International Conference on Information Fusion (FUSION)*, 1-8
8. Jones B., Delande E., Zucchelli E., and Jah M., (2019). Multi-Fidelity Orbit Uncertainty Propagation

with Systematic Errors, *Proceeding of The Advanced Maui Optical and Space Surveillance Technologies Conference (AMOS), Maui HI*

9. Nakamura E., Loureiro A., and Frery A., (2007). Information fusion for wireless sensor networks: Methods, models, and classifications, *ACM Computing Surveys (CSUR)*, **39**(3) 9-es

10. Gu D., Sun J., Hu Z., and Li H., (2008). Consensus based distributed particle filter in sensor networks, *2008 International Conference on Information and Automation*, 302–307

11. Fantacci C. and Papi F., (2016). Scalable Multisensor Multitarget Tracking Using the Marginalized δ-GLMB Density, *IEEE Signal Processing Letters*, **23**(6) 863-867

12. Battistelli G., Chisci L., Fantacci C., Farina A., and Graziano A., (2013). Consensus CPHD filter for distributed multitarget tracking, *IEEE Journal of Selected Topics in Signal Processing*, **7**(3) 508-520

13. Farahmand S., Roumeliotis S., and Giannakis G., (2011). Set-membership constrained particle filter: Distributed adaptation for sensor networks, *IEEE Transactions on Signal Processing*, **59**(9), 4122-4138

14. Mohammadi A. and Asif A., (2011). Consensus-based distributed unscented particle filter, *2011 IEEE Statistical Signal Processing Workshop (SSP)*, 237-240

15. Gu D., (2007). Distributed particle filter for target tracking, *Proceedings 2007 IEEE International Conference on Robotics and Automation*, 3856-3861

16. Li, J. and Nehorai A., (2017). Distributed particle filtering via optimal fusion of Gaussian mixtures, *IEEE Transactions on Signal and Information Processing over Networks*, **4**(2) 280-292

17. Li W., Wei G., Han F., and Liu Y., (2015). Weighted average consensus-based unscented Kalman filtering, *IEEE transactions on cybernetics*, **46**(2) 558-567

18. Dubois D., and Prade H., (2015). Possibility theory and its applications: Where do we stand? *Springer handbook of computational intelligence*, 31-60

19. Rudolph V., Arnaud D., Nando D.F., Eric W., (2001). The unscented particle filter, *Advances in neural information processing systems*, 584-590

20. Raihan D., and Chakravorty, S., (2018). Particle Gaussian mixture filters-I, *Automatica*, **98** 331-340

21. Raihan D., and Chakravorty, S., (2018). Particle Gaussian mixture filters-II, *Automatica*, **98** 341-349

22. Cai H. and Jah, M., (2021). Credibility Filter for Space Object Tracking, *Submitted to Journal of Guidance, Control, and Dynamics*

23. Olfati R., Fax A., and MurrayR., (2007). Consensus and cooperation in networked multi-agent systems, *Proceedings of the IEEE*, **95**(1), 215-233

24. Beard M., Vo B.T., Vo, B.N., Arulampalam S., (2017). Void Probabilities and Cauchy–Schwarz Divergence for Generalized Labeled Multi-Bernoulli Models, *IEEE Transactions on Signal Processing*, **65**(19) 5047-5061

25. Wang X., Hoseinnezhad R., Gostar A., Rathnayake T., Xu B., and Bab-Hadiashar A., (2017). Statistical Information Fusion for Multiple-View Sensor Data in Multi-Object Tracking. *arXiv preprint arXiv:1702.08641*

26. Cai H., Gehly S., Yang Y., Hoseinnezhad R., Norman R., and Zhang K., (2019) Multisensor Tasking Using Analytical Rényi Divergence in Labeled Multi-Bernoulli Filtering, *Journal of Guidance, Control, and Dynamics*, **42**(9) 2078-2085

27. Higashi M. and Klir G., (1982). Measures of uncertainty and information based on possibility distributions, *International journal of general systems*, **9**(1) 43-58

28. Higashi M. and Klir G., (1983). On the notion of distance representing information closeness: Possibility and probability distributions, *INTERNATIONAL JOURNAL OF GENERAL SYSTEM*, **9**(2) 103-115

29. Cai H., Yang Y., Gehly S., Wu S., Zhang K., (2018). Improved tracklet association for space objects using short-arc optical measurements, *Acta Astronautica*, **151** 836-847